Aerodynamic Design of Radial Inflow Turbine for Medium Scale Organic Rankine Cycle System

Lei Chen, Boaz Habib, Nick Inskip

Industry Development Division, Heavy Engineering Research Association, New Zealand

lei.chen@hera.org.nz

Keywords: *Radial inflow turbine, organic rankine cycle, aerodynamic design, numerical simulation*

ABSTRACT

The Organic Rankine Cycle (ORC) has been considered to be the most feasible technology among the existing approaches to convert low grade heat source (such as geothermal energy) and industrial waste heat into electricity. For a medium scale ORC system with a general power range of 50kW to 500kW, radial inflow turbines, with low mass flow rate and high pressure ratio, are applied more often than other types of turbines, because they are more efficient, adaptable, stable and cost-effective. When developing such a turbine, aerodynamic design is a step of vital importance. This paper presents a complete aerodynamic design process of a 50kW radial inflow turbine, including preliminary design, three dimensional modelling of the blades and volute, and three dimensional numerical simulation. The preliminary design is carried out by using ANSYS RTD, which can effectively generate an optimal solution whilst fixing the values of mass flow rate, pressure ratio and blade speed ratio. Subsequently, based on the preliminary design results, the cascade shape modelling of the stator and the rotor is conducted through in-house code and ANSYS BladeGen respectively. Afterwards, the three dimensional modelling of the stator and the rotor is conducted by stacking the cascades along a specified line. The volute is defined by a series of radial circular sections on the periphery of the turbine and the radii of the sections are obtained through the free vortex theory. ANSYS DesignModeler is used to perform three dimensional modelling of the volute. Finally, three dimensional numerical simulation of the radial inflow turbine is carried out by employing ANSYS TurboGrid, ICEM and CFX, where, in this case, R245fa was used as the working fluid. Detailed analyses of the flow field across the turbine stage and the volute are presented and the performance assessment of the turbine in terms of efficiency, mass flow rate and optimum speed ratio is illustrated.

1. INTRODUTION

New Zealand has extensive renewable energy resources (such as hydro, geothermal, wind and marine), which are beneficial to economic development, environmental protection and energy security. Globally, nations are making great effort to improve energy security, reduce pressure on the environment and reduce greenhouse gas emissions.

Among the projects proposed to make use of renewable energy in New Zealand, Above Ground Gerthermal and Allied Technologies (AGGAT) involves all aspects of above ground technologies based on geothermal and/or other allied heat sources by using Organic Rankine Cycle (ORC) technology. The programme uniquely brings together researchers, industry and international partners on a collaborative platform; drawing on their expertise in research, fabrication, knowledge and experience to deliver new AGGAT products.

The contents of research and development work of the AGGAT programme are presented via the AGGAT diamond, shown in Figure 1. The programme focuses on:

- Renewable energy sources such as geothermal, waste heat, solar thermal etc
- Energy conversion technologies such as ORC / Kalina
- Scales of operation from lab through to commercial stage
- Effective means of new technology integration into existing processes

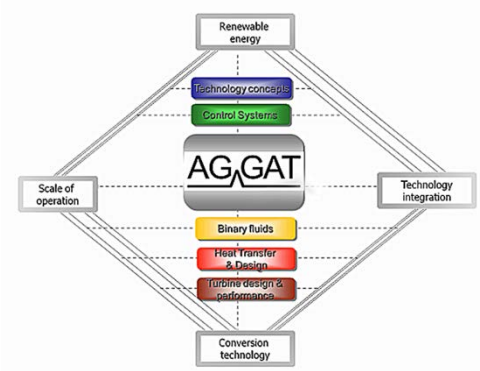

Figure 1: Framework of AGGAT programme

By integrating all the technologies above, the AGGAT programme aims at achieving sustainable economic development through the efficient use of energy resources with the ultimate goal of working towards a 'responsible' future.

Among the existing approaches of using geothermal resources, the ORC is considered to be the most feasible one to convert low grade heat sources and industrial waste heat into electricity. The ORC technology is of crucial importance in the power system (Quoilin, Van Den Broek, & Declaye, 2013):

- It can have a beneficial effect on the energy intensity of industrial processes, mainly by recovering waste heat.
- It can have a positive effect on building consumptions, e.g. using Combined Heat Power systems.
- It can be used to convert renewable heat sources into electricity.

The Organic Rankine Cycle also shows a number of advantages over the steam cycle (Quiolin, Orosz, & Hemond, 2011): a lower working temperature, the absence of droplets during the expansion the low maintenance requirements as well as relative simplicity. According to the Schuster's study (Schuster, Karellas,& Kakaras, 2009), Organic Rankine Cycle applications have economic attractiveness when used at small and medium power scales. This is the basis behind the AGGAT programme's focus on ORC technology.

The ORC system is presented in Figure 2, and it consists of four processes:

- 1-2: Compression of the organic fluid in the pump. The saturated fluid from the condenser is compressed and pumped into the evaporator;
- 2-3: Vaporization of the organic fluid in the evaporator. The working fluid absorbs the heat from the geothermal or waste heat source and vaporizes into a saturated vapour.
- 3-4: Expansion of the organic fluid in the turbine.
- 4-1: Isobaric condensation of the organic fluid in the condenser.

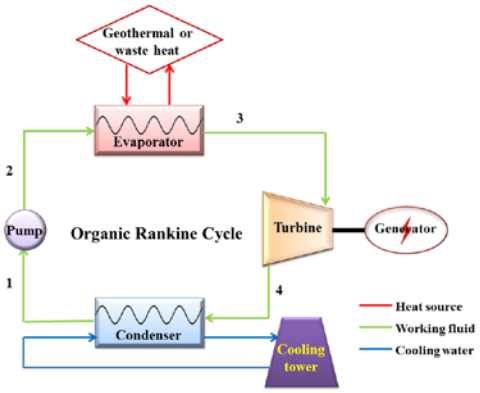

Figure 2: Organic Rankine Cycle system

In an ORC system, the turbine or expander has a substantial effect on the performance. Specification of the turbine technology of choice depends on the operating conditions and the size of the given system. A radial inflow turbine is adopted in this study as it is suitable for medium scale power generation (50kW-500kW) with low mass flow rate and high pressure ratio, as well as other motivations (Sauret, Rowlands, 2011): Radial inflow turbines require minor modifications for different geothermal resources; it is less sensitive to blade profile inaccuracies than axial turbines and more robust under increased blade load caused by using high-density fluids at subcritical or supercritical conditions; Radial inflow turbines are easier to manufacture compared to axial machines as the blades are attached to the hub; The rotor-dynamic stability of radial inflow turbine is also improved due to a higher stiffness.

Therefore, for the development of the AGGAT turbine with 50kW power output, a single stage radial inflow turbine design was chosen, using R245fa as the working fluid, due to its environmental characteristics, cost-effectiveness, thermal stability and properties (Bertrand, Papadakis, & Lambrinos, 2013; Liu, Chien,&Wang, 2004; Lopez, 2013), to convert the heat energy into the mechanical energy in the ORC system.

When developing such an AGGAT radial inflow turbine, aerodynamic design is a vital step in the turbine design system which consists of aerodynamic design, stress analysis, rotor dynamics analysis, manufacture and testing. Thus, this paper presents the details of the aerodynamic design from 1D preliminary design to 3D modeling of turbine blades, passage and volute, and provides the analysis of flow field and performance under the design point and non-design point.

2. AERODYNAMIC DESIGN SYSTEM OF TURBINE

The aerodynamic design includes five components which are 1D preliminary design, blade profile and passage design, 3D geometry of blade and passage, 3D modeling of volute and 3D numerical simulation, as shown in Figure 3.

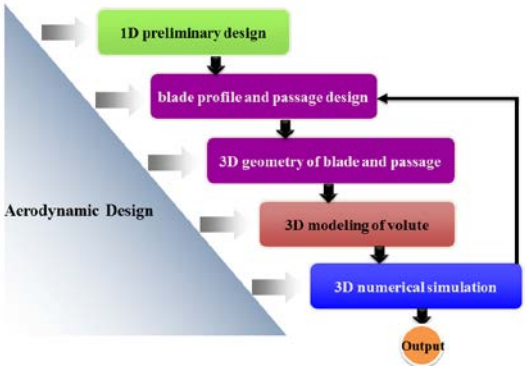

Figure 3: Aerodynamic design system of turbine

In the aerodynamic design system, 1D preliminary design is firstly carried out to get well-matched flow conditions, especially the flow angles at inlet and outlet of the stator and the rotor. The basic dimensions of the blades and passage are established in the preliminary design as well, which initiates the detailed aerodynamic design of the turbine. The other four components, which follow the 1D preliminary design, are detailed design stages. The aim is to find the optimum design solution of turbine with the highest efficiency. Based on the results from the 1D preliminary design, the blade profiles from the root section to the tip section are normally constructed by using two approaches, which are direct profile design method and camber line plus thickness method. For the direct profile design method, the blade profile is directly constructed by utilizing a multi-order function (mostly third order), such as Bezier function with four control points. While, the camber line plus thickness method is performed by using multi-order Bezier function or spline function. When given the thickness distribution, the blade profile is easily built based on the geometric relations between the adjacent inscribed circles. After that, 3D geometry of the blade is generated by stacking the blade profiles from root section to tip section and 3D modeling of the volute is completed by employing the free vortex theory based on the dimension and the flow conditions at the stator inlet. Finally, it goes to the 3D numerical simulation, which is to evaluate the performance of turbine including efficiency, power, mass flow rate and pressure ratio et al. The next design cycle is initiated until an optimum solution is achieved.

2.1 1D preliminary design

In the 1D preliminary design, a set of stations is chosen at the inlet of every component of the turbine (volute, stator and rotor). Given the appropriate value of aerodynamic and thermodynamic parameters (mass flow rate, pressure ratio, flow angles, fluid properties et al.), the thermodynamic and fluid dynamic conservation principles are applied at each station and the equations involved are solved through the iteration method, subject to estimated levels of loss and efficiency. After that, the results including the basic geometric dimensions (blade heights, dimensions of inlet and outlet for stator and rotor, axial length of blade et al.) and aerodynamic parameters (power, flow angles at inlet and outlet of each component, Mach number et al.) under the design point are output for the detailed design in the following step.

For a good preliminary design of a radial inflow turbine, there are two core correlations that should be used during the design, they are: optimum speed ratio, specific speed and specific diameter

The optimum speed ratio plays a crucial role in the preliminary design of radial inflow turbine (Dixon, Hall, 2013; Barr, Spence, & Eynon, 2008; Shahhosseini, Hajilouy, & Rad, 2008; Wong, Krumdieck, 2014), which is defined as,

$$\frac{U}{C_0} = \frac{U}{\sqrt{2\Delta h_{is}}} \quad (1)$$

where U (m/s) is the tip speed of rotor and C_0 (m/s) is called spouting velocity. Spouting velocity is the velocity that has an associated kinetic energy equal to the isentropic enthalpy drop Δh_{is} from turbine inlet stagnation pressure to the final exhaust pressure. The optimum speed ratio is mainly used to evaluate turbine performance under the non-design point, as shown in Figure 4. Generally, the optimum speed ratio is equal to about 0.7 for the turbine under the design point.

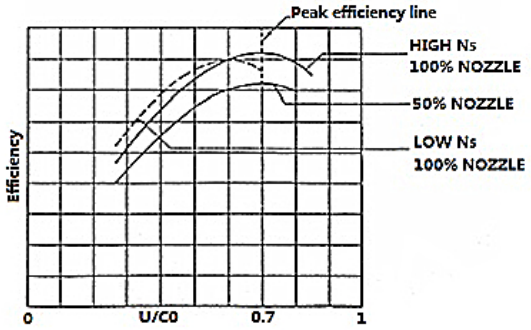

Figure 4: Relations between efficiency and optimum speed ratio (Marcuccilli, Zouaghi, 2007)

The application of specific speed N_s and specific diameter D_s was also proposed for the radial inflow turbine design (Cordier, 1955; Balje, 1981; Wright, Gerhart, 2010; Ventura, Jacobs, Rowlands, 2012). They are applied to correlate the performance of radial inflow turbine to a wide range of specific speed and specific diameter. Both of the specific speed N_s and specific diameter D_s are non-dimensional parameter. N_s is mainly used to define the rotational speed of radial inflow turbine and D_s is the one to represent the characteristics diameter of turbine. The expressions are,

$$N_s = \frac{\omega\sqrt{m/\rho_{exit}}}{\Delta h_{is}} \quad (2)$$

$$D_s = \frac{D(\Delta h_{is})^{0.25}}{\sqrt{m/\rho_{exit}}} \quad (3)$$

where, ω is rotational speed of turbine rotor, m is mass flow rate across the turbine stage, ρ_{exit} is fluid density at the turbine outlet, Δh_{is} is isentropic enthalpy drop from the inlet to the outlet and it is the same as that of equation (1), and D is diameter of turbine rotor. According to Figure 5, the optimum ranges of specific speed and specific diameter are (0.4-0.9), (3-5) respectively.

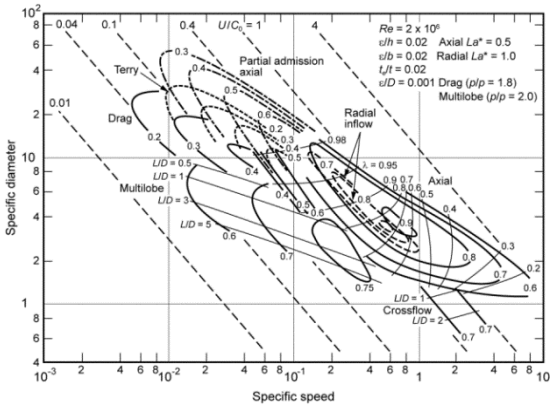

Figure 5: Turbine performance chart as a function of specific speed and specific diameter (Balje, 1981)

All the correlations (optimum speed ratio, specific speed and specific diameter) illustrated above are the core parameters during the radial inflow turbine design and these correlations are compatible with each other. It means that a good turbine design can be achieved based on any of the correlations.

Based on the correlations and expressions, the 1D preliminary design is conducted by using the ANSYS Radial Turbine Design (RTD) module. By setting the aerodynamic and geometric parameters (such as inlet total pressure, inlet total temperature, mass flow rate, pressure ratio, optimum speed ratio, rotational speed, inlet absolute flow angle, ratio of rotor exit tip to inlet radius, ratio of rotor exit hub to inlet radius and number of rotor blades) for RTD, the turbine performance data is obtained as presented below.

- Optimum speed ratio: 0.695
- Specific speed: 0.45
- Isentropic efficiency: 0.868
- Power: 60.5kW
- Rotor exit absolute flow angle: 0^o

2.2 3D modeling of turbine

This chapter presents the detailed design step for the AGGAT turbine based on the results from the 1D preliminary design. It includes the design method of the stator, rotor and volute, and the numerical simulation of turbine as well as the analyses of the turbine flow field.

2.2.1 Design method of turbine blades and passage

For the stator design, an in-house code is adopted to carry out the modeling of turbine stator in this section. The code is developed based on the camber line plus thickness method, illustrated in Figure 6. This method uses a third-order spline function for constructing the camber line and the thickness based on the flow angles calculated from the 1D preliminary design. Given the thickness distribution, the stator cascade is formed on the basis of the geometric relations between the adjacent inscribed circles. The stator passage width is constant and is identical to the rotor inlet blade height determined from the rotor sizing.

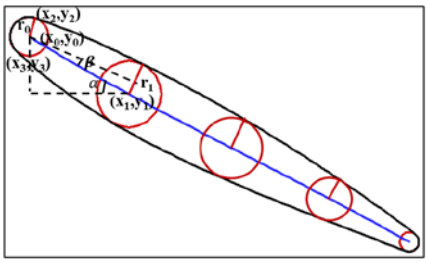

Figure 6: Design method of turbine stator

For the rotor design, the ANSYS BladeGen module, which is a geometry creation tool specialized for turbomachinery blades and passages, is used to perform the modeling of turbine rotor in this section. Figure 7 shows the detailed information of the BladeGen for the radial inflow turbine design. The passage is designed using Fourth-order Bezier curve based on the passage dimension from the 1D preliminary design and the rotor cascade is constructed through the camber line plus thickness method. The camber line angle Theta can be adjusted to change the expansion level of the fluid and the flow angle in order to ensure that the flow condition is good enough in the rotor passage and the absolute flow angle is about zero at the rotor outlet, leading the fluid to exit in the axial direction.

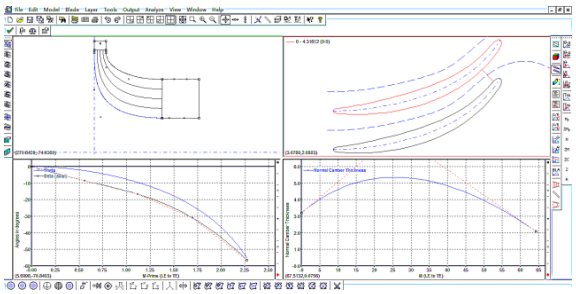

Figure 7: Rotor design using BladeGen

2.2.2 Design method of turbine volute

A turbine volute is a unique component in turomachinery that leads the fluid to enter into the stator passage.
When performing the design of the volute, it should be ensured that there is a uniform flow in the volute passage to reduce the flow loss. The fluid goes along the volute passage, while entering into the stator passage.

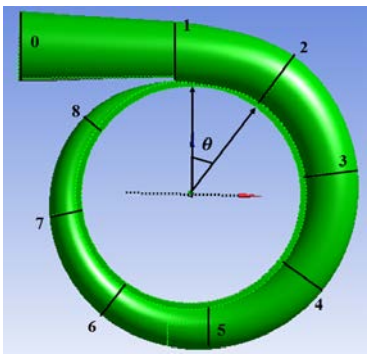

Figure 8: Volute sections

To obtain a uniform flow field in the volute passage, its section area should decrease gradually from the inlet to the tongue along the stream wise direction as shown in Figure 8.

The volute has four typical section shapes, which are rectangle, circle, ellipse and trapezium. In this study, the circular section shape is adopted for the volute design (see Figure 9). The volute is defined by a series of radial sections on the periphery of the turbine and the modeling of the circular sections is carried out by using the continuity and angular momentum theory.

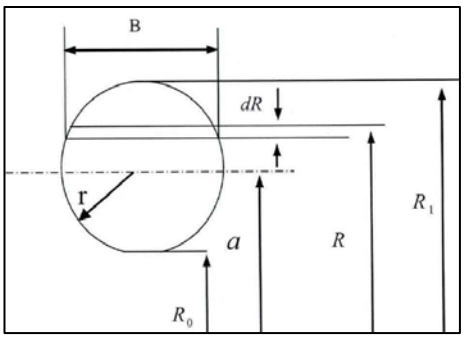

Figure 9: Circular section of volute

The assumptions are,

- The density of the fluid is constant in the volute and it is equal to the density at the volute inlet.
- The flow loss is neglected in the passage and it is the free vortex flow for the fluid, so it matches angular momentum, $c_u r = K = const$ where r is the radius of the circular section.

The design method of the circular section for volute is proposed by Xi (Xi, 2012) and the final expression of the circular section is,

$$c_u R_0 \rho_\theta 2\pi[R_0 + r - \sqrt{R_0(R_0+2r)}] = \frac{2c_r \rho \pi R_0 L(\theta_{\max} - \theta)}{\theta_{\max}} \quad (4)$$

where θ is the azimuth angle, G_θ is the mass flow rate, $c_{\theta u}$ is the tangential component velocity, ρ_θ is the density at the section, $\theta_{\max}$ is the maximum azimuth angle.

Based on the equation (4), the code for volute design is completed by using FORTRAN Language and then the sections from section 1 to section 8 can be obtained.For the section 0, which is the first circular section at the inlet of the volute and it has a great effect on the flow angle at the exit. The parameter A/a, which is the ratio of inlet area and the centroid radius, determines the flow angle at the volute exit (Baines, 2014), it has,

$$\tan\gamma = \frac{\mathrm{K}}{A/a} \quad (5)$$

where γ is the flow angle at the volute exit, K is the angular momentum.

After obtaining all the circular sections, the 3D modeling of the volute is conducted by using the ANSYS DesignModeler based on the Parameters Setting function in ANSYS CPD module.

The 3D geometry of the AGGAT radial inflow turbine is shown in Figure 10.

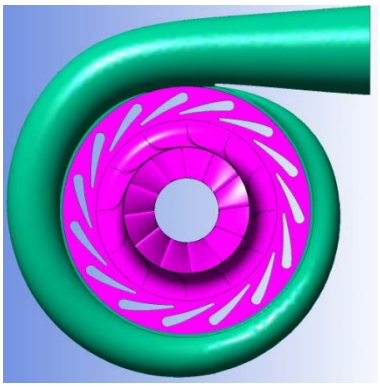

Figure 10: 3D geometry of AGGAT turbine

2.3 3D simulation of turbine under the design point

To save the calculation time and reduce the period of aerodynamic design, the numerical simulations of the turbine blades for single passage and the volute are performed separately.

2.3.1 Simulation of turbine blades and passage

The numerical simulation of the turbine blades and passage is conducted by using ANSYS CFX and TurboGrid. The Shear-Stress-Transport (SST) turbulence model is adopted due to its accurate predictions of flow separation (Menter, 1994).

The mesh and the boundary condition for the simulation are presented in Figure 11. The total mesh nodes are 994780 with mesh refinement near the wall to calculate the viscous loss accurately in the boundary layer. The total pressure, the total temperature and the flow angle are set at the inlet boundary conditions. It is the periodic condition for the boundary of the stator passage and the rotor passage, and the stage mixing plane model is used at the interface between the stator and the rotor. The wall boundary condition is proposed for the blade and the passage wall, and the static pressure is set at the rotor outlet.

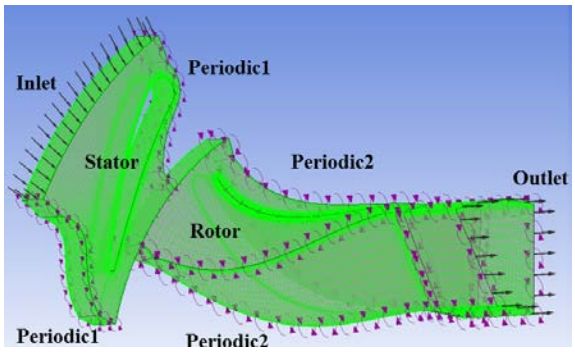

Figure 11: Mesh and boundary condition for numerical simulation

Aungier Redlich Kwong model (Aungier, 2006) is chosen for predicting the real gas properties of R245fa by using the Fourth Order Polynomial coefficients for the heat capacity at constant pressure.

The performance data of the radial inflow turbine under the design point from the numerical simulation is shown in Table 1. The optimum speed ratio, specific speed and specific diameter are 0.704, 0.46 and 4.45 respectively and all of them are within the optimum ranges mentioned in Chapter 2.1, implying that the aerodynamic design is good.

Table 1. Turbine performance from 3D simulation

Power (kW)	Optimum speed ratio	Specific speed	Specific diameter	Isentropic efficiency (t-t)
54.6	0.704	0.46	4.45	0.8597

It is crucial to ensure that the working fluid is at the vapour state during the expansion process in the turbine and the temperature-entropy diagram (Kang, 2012) is a proper choice to observe the state values by locating the expansion, as shown in Figure 12. The temperature-entropy diagram illustrates the state of the working fluid R245fa during the expansion process across the turbine. As it can be seen, the expansion process of the fluid from the design takes place at the superheated vapour zone and it is close to the saturated vapour line.

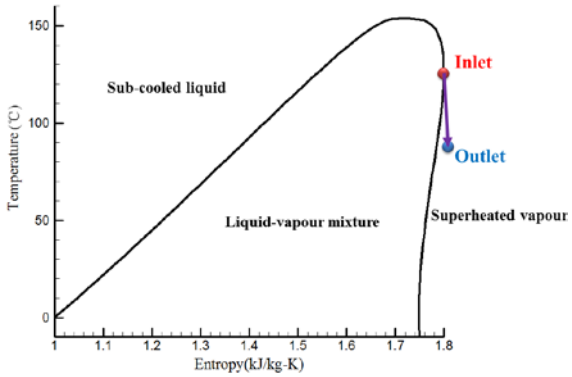

Figure 12: Temperature-entropy diagram for R245fa

The detailed analyses of the flow field are conducted to evaluate the turbine performance in the following.

Figure 13 shows the streamlines distribution in the turbine passage. The streamlines go smoothly from the inlet to the outlet without obvious separation, which indicates a good flow condition in the stator passage. While, in the rotor passage, the tip leakage flow goes from the pressure side to the suction side and mixes with the main stream. The mixed separation flow dominates most of the passage at about 30% axial length of the blade chord causing massive secondary flow loss.

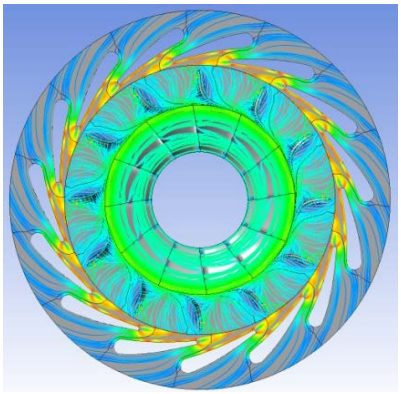

(a) Full passage

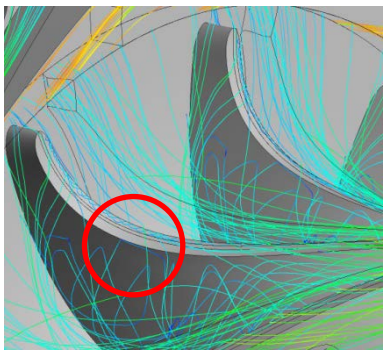

(b) Rotor passage

Figure 13: Streamlines distribution in turbine passage

The most effective approach to reduce the tip leakage flow is to reduce the tip clearance, which has been reduced to 0.4 mm in this study, and the secondary flow loss will be decreased if the tip clearance is reduced further to 0.3 mm, however, manufacturing tolerance must be considered.

Figure 14 shows the static pressure contour on the hub and the blades. The pressure distribution on the hub and the blade of the stator is uniform and it presents good flow features. However, the pressure contour of the rotor is not as good as that of the stator. At the suction surface, the static pressure is not uniform along the stream wise and radial direction caused by the strong tip leakage flow shown in Figure 13.

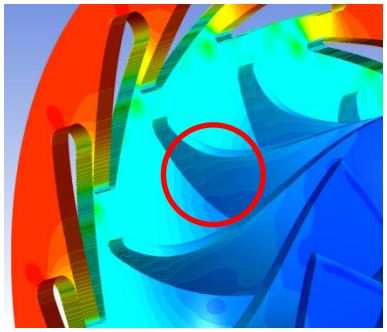

Figure 14: Static pressure contour on hub and blades

The relative and absolute flow angles at the leading edge and the trailing edge of the rotor are shown in Figure 15. The blue line Alpha represents the absolute flow angles and the red line Beta represents the relative flow angles. From the image (a), the averaged values of the relative flow angles (incidence angles) are -22.5 degrees at the leading edge, and it is within the optimum range from -15 to -30 degrees for a good design of radial inflow turbine (Logan, 2003; Baines, 2003). The averaged absolute flow angles are 76.2 degrees at the leading edge. As the image (b) shows, the averaged absolute flow angles at the trailing edge from the hub section to 30% span section are 6.0 degrees and it flows out nearly in axial direction, while the flow angle increases greatly from the 30% span section to the 60% span section reaching about 45 degrees and then it drops a little bit to about 35 degrees. The dramatic changes in the outlet absolute flow angles from 30% span section to the tip section is caused by the strong tip leakage flow and it means that the separation flow has a huge negative effect on both the main stream and the power output.

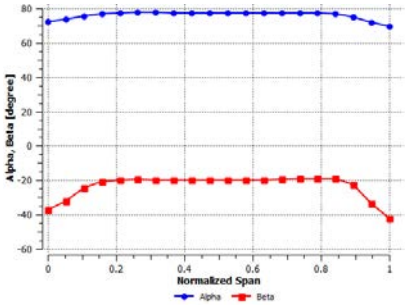

(a) Leading edge

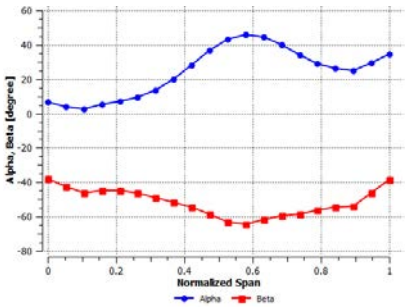

(b) Trailing edge

Figure 15: Distribution of the flow angles at the leading edge and trailing edge

2.3.2 Simulation of volute

ANSYS CFX and ICEM are employed for the simulation of volute. The SST turbulence model is used and the boundary condition and mesh for the simulation are shown in Figure 16. The total pressure and the total temperature are set at the inlet boundary condition with the flow direction perpendicular to the inlet boundary surface. The wall boundary condition is proposed for the volute passage, and the static pressure is set at the outlet. The total mesh elements of volute are 403230.

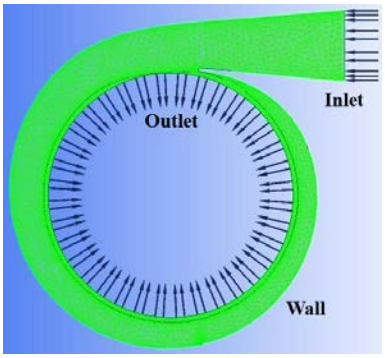

Figure 16: Mesh and boundary condition for volute simulation

The streamlines distribution in the volute passage is presented in Figure 17. It shows an excellent flow condition of the working fluid in the volute passage from the inlet to the outlet without any separation, indicating the effectiveness of the volute design method (the continuity and angular momentum theory). The working fluid enters into the volute passage at the inlet and goes along the passage to the tongue with a uniform flow field.

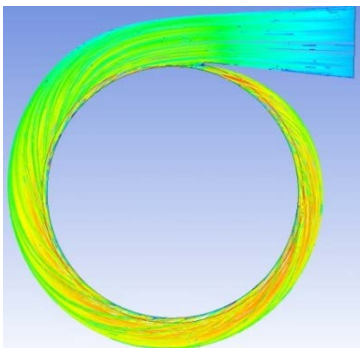

Figure 17: Streamlines in the volute passage

Figure 18 shows the static pressure contour on the volute passage. It can be seen that the static pressure decreases smoothly from the inlet to the outlet without obvious low pressure value zones. In addition, as the flow area decreases gradually from the inlet to the outlet, the velocity increases. In this way, the mass flow rate is kept constant. Thus, the pressure is relatively low at the outlet. Overall, the flow efficiency is high in the volute passage.

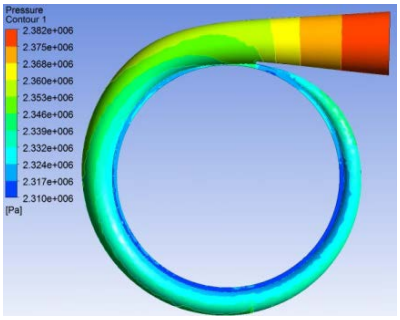

Figure 18: The static pressure contour on the volute passage

2.4 3D simulation of turbine under the non-design point

The optimum speed ratio and efficiency curve is presented in Figure 19. As the image shows, the turbine efficiency increases with the increase of the optimum speed ratio, peaking before starting to drop off at a speed ratio of 0.75. The efficiency stays higher than 0.75 in the wide range of optimum speed ratios from 0.54 to 0.98. The efficiency at the design point is 0.8597 with the optimum speed ratio of 0.704, while the highest efficiency is 0.8643 with the optimum speed ratio of 0.75. The high efficiency zone (higher than 0.86) is within the optimum speed ratio range from 0.7 to 0.8.

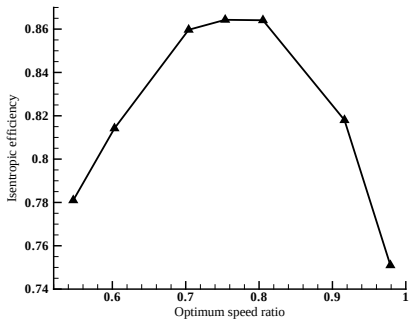

Figure 19: Optimum speed ratio and efficiency curve

Figure 20 shows the mass flow rate and total-total pressure ratio curve. From the image below, the mass flow rate increases with the rise of total-total pressure ratio and reaches the choked value (maximum value) at the total-total pressure ratio under the design point. Then the mass flow rate stays constant even as the pressure ratio continues to increase. To produce more power, the turbine from the design is operating at the choked mass flow rate with a high isentropic efficiency of about 0.8597.

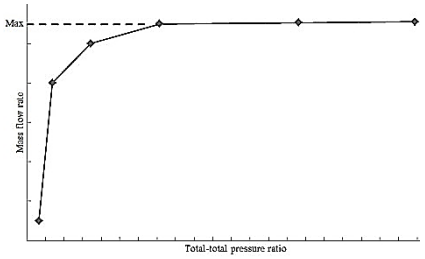

Figure 20: Mass flow rate and total-total pressure ratio curve

3. CONCLUSION

From 1D preliminary design to 3D modeling, this paper presents a detailed aerodynamic design approach for a radial inflow turbine in an Organic Rankine Cycle system using R245fa as the working fluid. The in-house code and the ANSYS turbomachinery module are used to conduct the turbine design based on correlations surrounding optimum speed ratio, specific speed and specific diameter. Under the design point, the power of the turbine is 54.6 kW and the isentropic efficiency is 0.8597. The strong tip leakage flow of the rotor mixes with the main stream and the mixed seperation flow dominates most of the passage at about 30% axial length of the blade chord. It causes massive secondary flow loss and increases the absolute flow angle greatly at the rotor exit, which substantially impacts the power output. The flow condition in the volute passage is excellent without any separation. Under the non-design point, the turbine efficiency stays higher than 0.75 in the wide range of optimum speed ratios from 0.54 to 0.98 and the mass flow rate increases with the rise of total-total pressure ratio and reaches the choked value where it remains unchanged with further increases in pressure ratio.

The stress analysis and rotor dynamics analysis of the turbine will be conducted in the next few months, and the turbine will be tested to validate the simulations results in the pilot plant next year.

ACKNOWLEDGEMENTS

This work was part of the AGGAT programme funded by NZ Ministry for Business Innovation and Employment. The authors would like to thank the ORC research team in HERA for their helpful feedback. The authors would also like to thank Brent Young and Wei Yu for the access to ANSYS software.

REFERENCES

Aungier, R.H., Turbine aerodynamics: axial-flow and radial-inflow turbine design and analysis.ASME Press. (2006).

Baines N C, Japikse D. Axial and radial turbines [M]. Wilder, VT: Concepts NREC, 2003.

Baines, N. ENGR408-ENME 627-SI Special topic in engineering: Turbomachinery. (2014).

Balje O E. Turbo-machinery: A Guide to design, Selection, and Theory [J]. (1981).

Barr L, Spence S W T, Eynon P. Improved performance of a radial turbine through the implementation of back swept blading[C]//ASME Turbo Expo 2008: Power for Land, Sea, and Air. American Society of Mechanical Engineers, 1459-1468. (2008).

Bertrand T F, Papadakis G, Lambrinos G, et al.: Criteria for working fluids selection in low-temperature solar organic Rankine cycles [C]//1st International Congress on Heating, Cooling and Buildings, Lisbon. (2013).

Cordier, O.. "Similarity considerations in turbomachines," VDI Reports, 3. (1955).

Dixon S L, Hall C. Fluid mechanics and thermodynamics of turbomachinery[M]. Butterworth-Heinemann. (2013).

Liu B T, Chien K H, Wang C C. Effect of working fluids on organic Rankine cycle for waste heat recovery [J]. Energy,29(8): 1207-1217. (2004).

Logan Jr E., Ramendra Roy. Handbook of turbomachinery [M]. CRC Press. (2003).

Lopez Sanz E. Study on a radial turbine stage with inlet guide vanes for an orc process with an electrical output of 3, 5 kW [J]. (2013).

Marcuccilli F, Zouaghi S. Radial inflow turbines for Kalina and organic Rankine cycles [J]. system, 2: 1.(2007).

Menter F R. Two-equation eddy-viscosity turbulence models for engineering applications [J]. AIAA journal, 32(8): 1598-1605. (1994).

Quoilin S, Orosz M, Hemond H: Performance and design optimization of a low-cost solar organic Rankine cycle for remote power generation [J]. Solar Energy, 85(5): 955-966. (2011).

Quoilin S, Van Den Broek M, Declaye S: Techno-economic survey of Organic Rankine Cycle (ORC) systems [J]. Renewable and Sustainable Energy Reviews, 22: 168-186. (2013).

Sauret E, Rowlands A S.: Candidate radial-inflow turbines and high-density working fluids for geothermal power systems [J]. Energy, 36(7): 4460-4467. (2011).

Schuster A, Karellas S, Kakaras E: Energetic and economic investigation of Organic Rankine Cycle applications [J]. Applied thermal engineering, 29(8): 1809-1817. (2009).

Kang S H. Design and experimental study of ORC (organic Rankine cycle) and radial turbine using R245fa working fluid [J]. Energy, 41(1): 514-524.(2012).

Shahhosseini M R, Hajilouy-Benisi A, Rad M. Numerical and Experimental Investigation of the Flow and Performance Characteristics of Twin-Entry Radial Turbine Under Full and Partial Admission Conditions[C]//ASME Turbo Expo 2008: Power for Land, Sea, and Air. American Society of Mechanical Engineers, 1507-1517. (2008).

Ventura C A M, Jacobs P A, Rowlands A S, et al. Preliminary design and performance estimation of radial inflow turbines: An automated approach [J]. Journal of Fluids Engineering, 134(3): 031102. (2012).

Wong C S, Krumdieck S. Energy and exergy analysis of an air-cooled geothermal power plant with fixed nozzle turbine subsonic expansion and supersonic expansion via CFD analysis[C]//Proceedings 36th New Zealand Geothermal Workshop, 24: 26. (2014).

Wright T., Gerhart Philip. Fluid machinery: application, selection, and design [M]. CRC press. (2010).

Xi Zhong. Investigation on aerodynamic design and optimization method for radial turbine [D]. Graduate University of Chinese Academy of Sciences (Institute of Engineering Thermophysics). (2012).